

EVALUATION OF THE BEHAVIOUR FACTOR BY INCREMENTAL DYNAMIC ANALYSES FOR THE SEISMIC DESIGN OF LIGHT-FRAME TIMBER BUILDINGS

Alessandra Gubana¹, Alessandro Mazelli¹

ABSTRACT: Light Frame Wood structures are today a valid alternative to Cross Laminated Timber structures for low and medium height buildings, both in terms of performance and environmental impact, given the lower volume of wood used. Light wood frames demonstrate a ductile behavior under seismic actions, linked to the plastic deformation of the connections, but uncertainties still regard the value of the behaviour factor associated to these types of structures.

This paper presents the evaluation of the behaviour factor 'q', used for the seismic design, based on Incremental Dynamic Analyses for Light-Frame Timber Buildings. Papers in literature regarding its evaluation are mostly based on static non-linear pushover analyses. Example buildings with 2, 3 and 4 storeys, were designed according to capacity design and then analysed by varying the displacement-ductility of the sheathing-to-frame connection. The results are then compared with the requirements provided by codes.

KEYWORDS: Light-frame timber buildings, Incremental Dynamic Analyses, Behaviour factor.

1 INTRODUCTION

Timber structures have a long tradition in several areas of the world, where residential balloon-frame and platform-frame houses constitute a large amount of the building stock. In the past, the carpenters' expertise drew the building construction process.

In the last years the use of timber in construction significantly developed, due to the growing attention to sustainability and environmental impact [1]. The appearance on the traditional market of new wood engineered products as Cross Laminated Timber (CLT) opened new technical possibilities and consequently also high multi-storey buildings can be built [2]. Thanks to prefabricated technologies, construction time can be strongly reduced with economic benefits on the real estate investment.

Light-frame wood (LFW) structures still represent a valid alternative to CLT structures for low and medium rise buildings, both in terms of performance and environmental impact, as the involved necessary timber mass is lower than in case of CLT. The advantages of the precast processes are also extended to LFW buildings, especially in Europe, where Light Frame Walls are built in prefabrication plants, often completed with the electrical and hydraulic systems and insulating materials and then connected in the building yards.

The good performance of timber buildings under earthquake excitations is well known and largely acquired, due to the limited mass and the high ductility ensured by, for instance, mechanical connections between sheathing to framing, wall to wall, wall to foundation.

Besides, hysteretic behaviour of LFW structures were investigated by means of tests on shake tables in past years. [3-5]

It is also well known that a reduction of seismic forces is possible due to the beneficial effects of energy dissipation in ductile structures and to inherent over-strength. This theoretical acquisition is considered in seismic design standards and codes, where force reduction factors (e.g. the 'behaviour factor' q in Eurocode 8 [6], or the 'response modification factor' R in US codes) are indicated to quantify the seismic design loads. The entity of these factors was initially based on empirical observations of the behaviour of common structural systems, but uncertainties still regard the value of q [7].

More recently, several numerical studies have been performed to determinate appropriate values, and most of them refer to non-linear static analyses results. A recent work by Rossi et al. [8] proposes the evaluation of q by static non-linear analysis, providing an important contribution to the calibration of the behaviour factor. However, static analysis does not consider the frequency of seismic input motion and the influence of higher vibration modes of the structure [9].

In the present work, a study for the evaluation of the behaviour factor q for LFW structures by means of Incremental Dynamic Analysis (IDA) is described.

Example buildings with 2, 3 and 4 storeys were designed according to capacity design and then analysed by varying the displacement-ductility of the panel. The results are then compared with the requirements provided by codes.

¹ DPIA Polytechnic Department of Engineering and Architecture, University of Udine (Italy).
alessandro.mazelli@uniud.it

2 LIGHT FRAME WOOD WALLS MODELLING AND VALIDATION

Light Frame Wood (LFW) shear walls are made up of timber-based panels (typically Oriented Strength Board OSB or plywood) and a timber frame connected together by small diameter nails. Angle brackets are used for shear forces at the base and the top of the panel, while hold-downs are placed at the corners to absorb tension and compression induced by bending moment.

Recent codes provide analytical methods to evaluate the stiffness or the top displacement of a LFW wall subjected to a horizontal force. The New Zealand standard [10], the American International Building Code IBC [11] and the Canadian Standard Association CSA O86 [12] consider the top displacement of a LFW wall as the sum of four terms: the base rotation δ_c , the shear deformation of the wood panel δ_s , the shear deformation of the sheathing-to-frame connection δ_{ps} and the bending deformation δ_b . The total displacement of the wall δ_w is evaluated by means of equation 1.

$$\delta_w = \delta_c + \delta_s + \delta_{ps} + \delta_b \quad (1)$$

It is worth noticing that the contribution due to the deformation of the angle brackets is not considered in equation 1. The slip is negligible only if the connectors are extremely stiff, consequence of a Capacity Design approach. Otherwise, it is always possible to add the base slip contribution to equation 1.

In order to assemble the example buildings with parameterized sheathing-to-frame connections, two wall FEM models were built: a detailed model (Figure 1a) and a simplified model (Figure 1b). Both were then calibrated thanks to the results of a cyclic test on a real scale LFW (3 m \times 3 m) Technical Report [13].

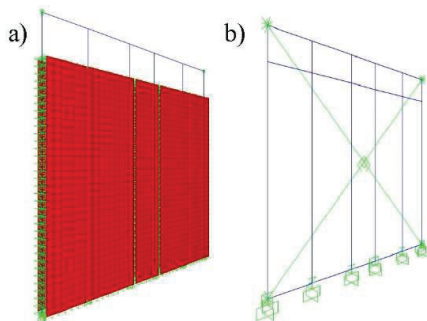


Figure 1: Analysis models of the wall: complete (a) and with equivalent non-linear springs (b).

The model of Figure 1a was built in SAP2000. OSB panel were modelled as *flat-shell* elements and timber studs as pinned *frames*. Non-linear links were used for hold-downs, angle brackets and for the nailed connection along the perimeter of the panels. It is worth noticing that the independent behaviour of the nail link in x and y directions leads to overestimate the strength of the connection in intermediate directions, and a squared rather than circular force domain is considered [14]. The

detailed model was validated through a pushover analysis (Figure 2). This model was then used to create the set of parameterized walls, varying the displacement ductility of the sheathing-to-frame connection.

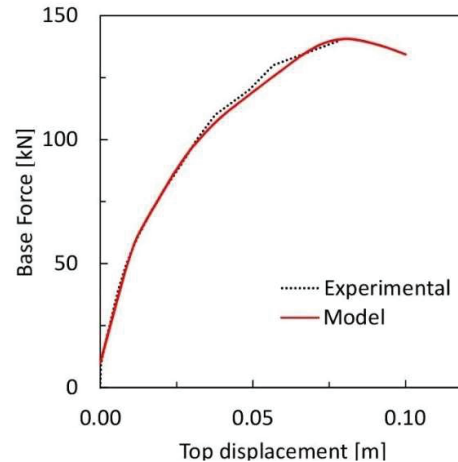


Figure 2: Comparison between experimental and analytical monotonic behaviour of the wall.

The model of Figure 1b was used to calibrate the pivot hysteresis parameters for non-linear uniaxial springs which represent the sheathing-to-frame connection, the hold-downs and the angle brackets separately. The walls were modelled by means of 5 non-linear springs each: two vertical springs for the hold-downs, one horizontal spring for the angle brackets and two inclined springs for the sheathing-to-frame connection. Their cyclic behaviour was validated by minimizing the difference with the experimental test in terms of dissipated energy (Figure 3). The simplified wall was then used in the modelling of the example buildings.

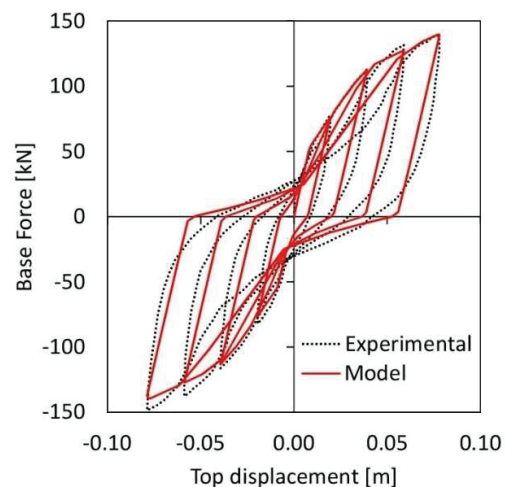


Figure 3: Comparison between experimental and analytical cyclic behaviour of the wall.

3 MULTI-STOREY TIMBER BUILDINGS

Example buildings with dimensions in plan of 6.50 m × 10.70 m with two up to four storeys, were built assembling 3 m × 3 m walls, in order to refer directly to the experimental test, and were calculated according to EN 1995-1-1:2005 [15] and EN 1998-1:2013 [6], following the Capacity Design (Figure 4). Each block can stand alone or be connected to other ones to have more surface area of the apartments.

The Life Safety ultimate state was verified by means of the Eurocode response spectrum with a PGA of 0.35 g, soil type A and q-factor equal to 3. The choice of q in the design procedure was necessary only to obtain realistic LFW wall structural dimensions, as the typical ones used in engineering design practice. The q equal to 3, in fact, affects the results only in term of resistance of the wall. The ductility of the nailed connection, in fact, will be parameterized. Furthermore, Rossi et al. [8] shows that the soil type has a negligible influence on the ductility evaluation.

An overstrength factor equal to 1 was chosen for the sheathing-to-frame connection, so that the nominal strength is equal to the design strength. On the other hand, hold-down and angle brackets were designed according to

the Capacity Design approach [16], with an overstrength factor of 1.6. Because of this choice, the contribute to dissipation of hold-down and angle brackets was not considered, as they were over strengthened, and all the plastic deformation were concentrated in the sheathing-to-frame connection. Each wall of the example buildings was modelled with the simplified method (Figure 1b).

4 PARAMETRIZATION OF LFW WALLS

Starting from the validate detailed model of Figure 1a, a set of LFW walls was created, varying the ductility of the sheathing-to-frame connection. Three classes were selected: 4, 6 and 8. The yield limit and the ductility of the nailed connection was evaluated according to an Equivalent Energy Elastic Plastic EEEP approach. Moreover, it was necessary to build set of walls that corresponds to the strength capacity required by the design procedure of the three example buildings. Thus, the connectors spacing and resistance was varied, and the OSB panels were placed on one or both sides. Table 1 reports the characteristics of the walls used to assemble the example buildings, obtained by means of pushover analyses.

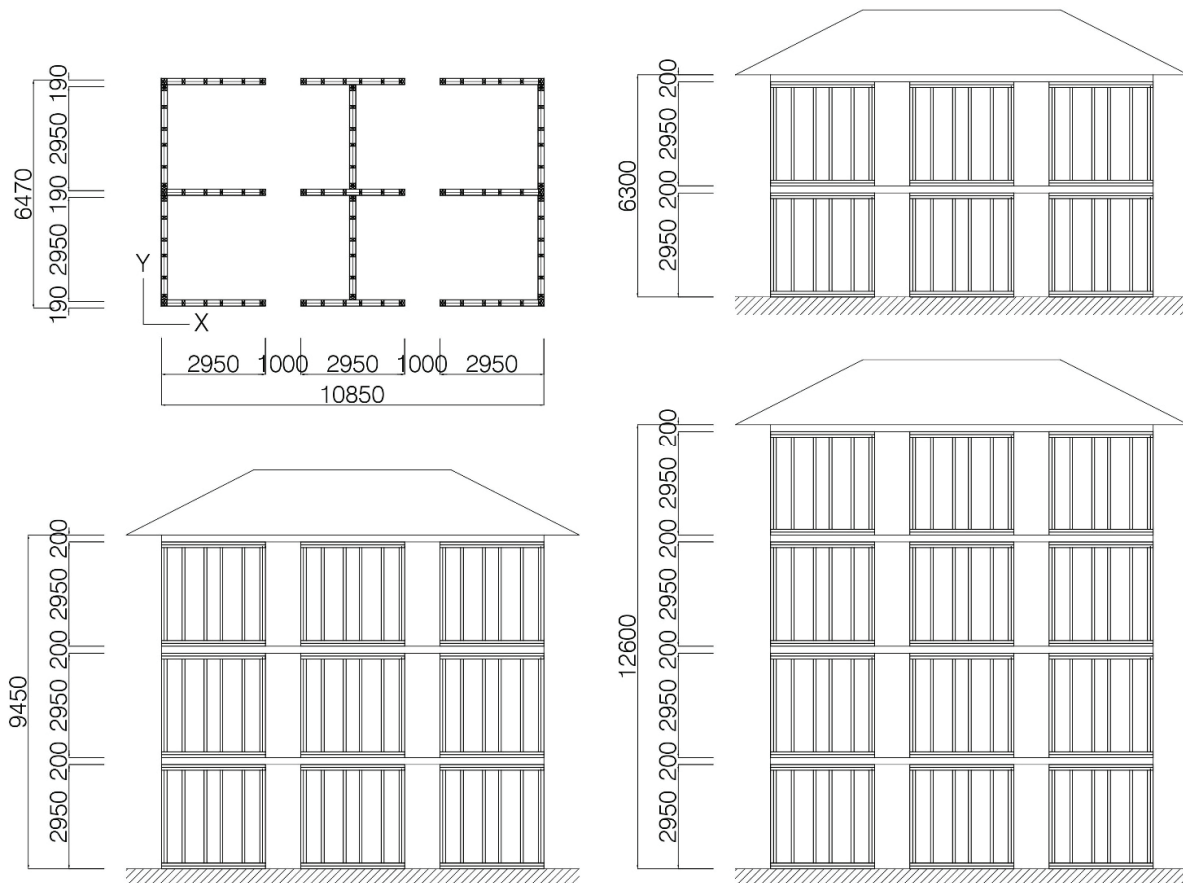


Figure 4: Example buildings (dimensions in mm).

F_{max} is the maximum resistant shear force of the wall, while d_y and d_u are the top horizontal displacement of the wall at yield and ultimate condition respectively. Each wall has a label that refers to the nail spacing (75 mm or 150 mm), the sides covered by OSB (1 or 2) and the resistance of the sheathing-to-frame connection, referred to only one nail (720 N or 1000 N).

Table 1: Parameterized walls used in the assembling of example buildings.

LFW connection ductility 4			
Wall type	F_{max} [kN]	d_y [m]	d_u [m]
75(1)720	23.1	0.015	0.037
150(1)720	11.2	0.012	0.036
75(1)1000	29.9	0.017	0.039
150(1)1000	18.6	0.014	0.042
150(2)1000	36.5	0.012	0.030
LFW connection ductility 6			
Wall type	F_{max} [kN]	d_y [mm]	d_u [mm]
75(1)720	25.6	0.017	0.058
150(1)720	12.3	0.013	0.048
75(1)1000	32.9	0.019	0.058
150(1)1000	20.6	0.015	0.055
150(2)1000	36.9	0.011	0.043
LFW connection ductility 8			
Wall type	F_{max} [kN]	d_y [mm]	d_u [mm]
75(1)720	27.0	0.019	0.077
150(1)720	12.7	0.014	0.062
75(1)1000	35.5	0.021	0.078
150(1)1000	21.7	0.016	0.072
150(2)1000	37.1	0.012	0.056

The increasing of the ductility of the sheathing-to-frame connection affects slightly F_{max} and d_y , while it influences widely d_u .

The pushover curves of each wall of each set were transformed into multilinear relationship. Then, the behaviour was adapted to the non-linear diagonal springs of the simplified models. The procedure is shown in Figure 5, where F and d are the shear force and the top displacement respectively. The subscript 45 refers to the 45° inclined spring.

Hysteretic pivot parameters of the sheathing-to-frame connection were already calibrated in section 2.

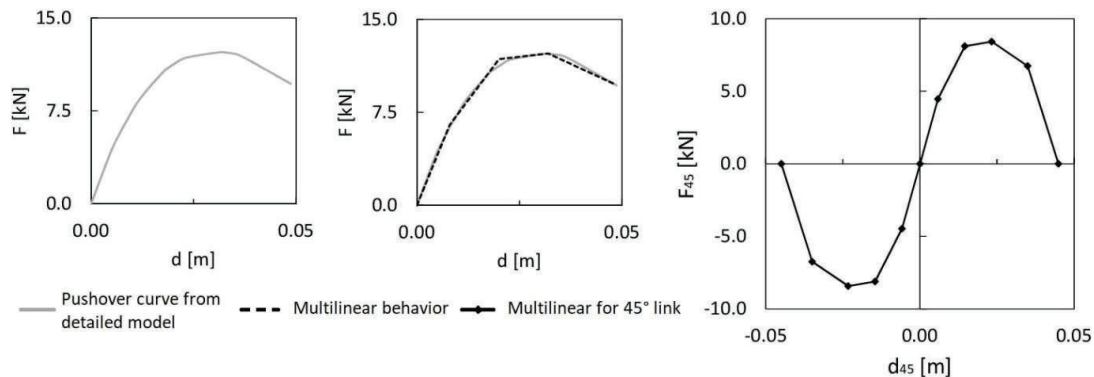


Figure 5: Procedure to obtain multilinear behaviour for uniaxial non-linear springs of the simplified LFW wall model.

An elastic behaviour was associated with hold-downs and angle brackets, since they were calculated according to the Capacity Design approach.

5 IDA PROCEDURE

The example buildings were analysed by means of IDA procedure [17].

The IDA consists in the execution of several non-linear dynamic analyses under a multiply scaled set of ground motion records. Every IDA curve represents the relationship between the Energy Demand Parameter (EDP) and the Intensity Measure IM. In the present study, the Peak Ground Acceleration (PGA) was chosen as IM and the ratio between the maximum roof displacement and the height of the building was selected as EDP (Mean Interstorey Drift Ratio MIDR). The choice of this couple (PGA, MIDR) allows to compare IDA curves at the same scale for each ductility class and for each number of storeys.

A set of 10 couples of records was chosen by means software REXEL [18] (Table 2).

Generally, the estimation of the q factor is obtained by means of non-linear static analysis via procedure present in the literature (e.g. Fajfar [19], Newmark and Hall [20]).

Table 2: Record selected for IDA procedure.

Earthquake name	Waveform ID	PGAX (m/s ²)	PGAY (m/s ²)
Friuli Earthq 1st shock	IT0014	3.39	3.09
L'Aquila Mainshock	IT0792	5.35	6.44
Campano Lucano	000291	1.53	1.73
Friuli (Aftershock)	000146	3.40	3.30
Kalamata	000414	2.35	2.67
Erzican	000535	3.81	5.03
Umbria Marche	000594	5.14	4.54
Montenegro	000196	4.45	3.00
South Iceland	004673	2.04	4.68
Bam (Iran)	000230	7.85	6.28

Several methods to evaluate q by means on non-linear dynamic analysis are available, considering experimental, numerical or hybrid procedures [21]. Some were already used for CLT buildings [22,23] In this work, a numerical method to evaluate q was chosen.

In fact, the behaviour factor q was obtained as the product of a ductility factor q_{μ} , connected to the non-linear behaviour of the structure, and an overstrength factor q_D , which takes into account the post-elastic hardening and the structural redundancy [24]:

$$q = q_{\mu} \cdot q_D \quad (2)$$

The obtained q is intrinsic and code independent, because the design overstrength factor for the sheathing-to-frame connection was set to 1.

The two factors of equation 2 follow the expression (3) and (4) respectively.

$$q_{\mu} = \frac{V_{b(Dyn,e)}}{V_{b(Dyn,y)}} \quad (3)$$

$$q_D = \frac{V_{b(Dyn,y)}}{V_{b(St,s)}} \quad (4)$$

where $V_{b(Dyn,y)}$ is the base shear which corresponds to the collapse of the structure, and $V_{b(Dyn,e)}$ is the base shear obtained by an elastic analysis of the structure under the same records. $V_{b(St,s)}$ is the base shear corresponding to the first yield in the structure and it is evaluated by means of a static non-linear analysis.

The use of non-linear static analysis avoids the problem of yield point detection. In fact, in an IDA, there could be more IM intensities with only one wall that has reached the yield displacement. This solution was used in other literature works [25,26].

It is worth noticing that the choice of IM and EDP did not affect the final results, since the q -factors were evaluated by base shear force ratios.

6 RESULTS

In this section, the result of the 90 IDA are reported.

Figure 6 illustrates two examples of wall reaching the ultimate displacement for a ductility class equal to 6, one in X direction and one in Y, according to Figure 4.

The diagrams show the relationship between the shear force on the wall F and its top horizontal displacement d . The sheathing-to-frame connection reaches the ultimate displacement under the scaled Kalamata earthquake for a $PGA = 0.13$ g. (Figure 6a). In Y direction, the wall attains to its ultimate displacement under the South Iceland accelerograms for a $PGA = 0.35$ g (Figure 6b).

In Figure 7 the complete IDA study is reported. The curves for each example building and for each ductility class are illustrated at the same scale, in order to perform comparison. Each graph shows the Mean Interstorey Drift Ratio versus the PGA.

On the basis of these first results, for a fixed ductility class, the MIDR shows a decreasing tendency when the number of storeys increases. On the other hand, the MIDR increases for higher ductility classes.

Finally, to a higher ductility class corresponds a higher average PGA at collapse.

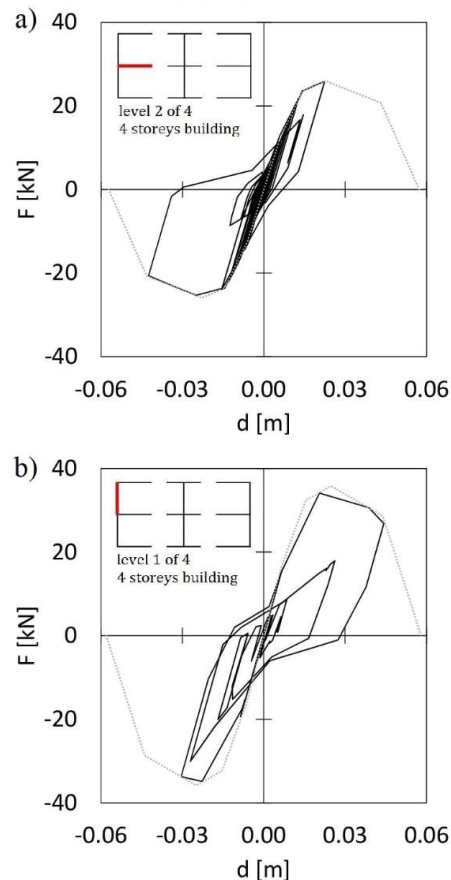


Figure 6: Hysteresis cycles for two walls attaining the ultimate displacement for a sheathing-to-frame connection ductility equal to 6 under Kalamata (a) and South Iceland (b) earthquakes.

Results of the IDA studies were used to evaluate the q factor, following equations 2, 3 and 4. Table 3 reports the minimum, mean and maximum values of the ductility factor q_{μ} , the overstrength factor q_D and the intrinsic factor q . Furthermore, the CoV is also reported for all the classes.

As expected, the ductility factor q_{μ} increases when increasing the ductility class of the sheathing-to-frame connection. Furthermore, the data are more scattered for higher values of ductility.

The overstrength factor q_D is higher as the ductility increases. Besides, the dispersion is lower with respect to the ductility factor.

The values of q reported in Table 3 are intrinsic and code independent. It can be noted that the value of 2.3 obtained for ductility class 6 correspond to the results reported in [8].

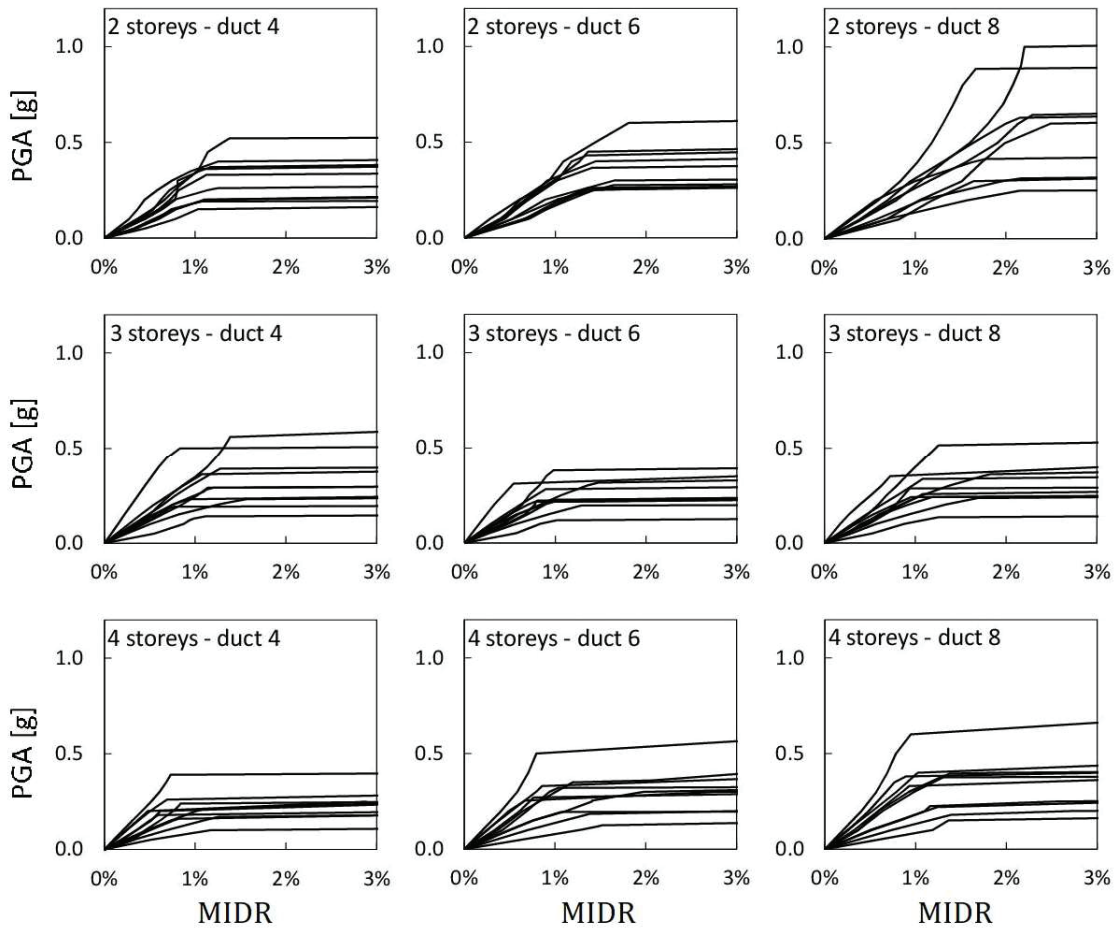


Figure 7: IDA study for each ductility class and for each building, representing the Mean Interstorey Drift Ratio (MIDR) vs the PGA.

Table 3: Ductility factor q_{μ} , overstrength factor q_D and intrinsic behaviour factor q for each ductility class and for each building.

LFW connection ductility 4												
	q_{μ}				q_D				q			
Storeys	2	3	4	global	2	3	4	global	2	3	4	global
Min	1.1	1.3	1.2	1.1	1.0	1.0	1.0	1.0	1.2	1.3	1.3	1.2
Mean	1.7	1.5	1.5	1.6	1.4	1.2	1.1	1.2	2.4	1.8	1.6	1.9
Max	2.3	2.3	2.9	2.3	1.6	1.3	1.3	1.6	3.6	2.2	2.3	3.6
CoV	0.22	0.18	0.22	0.19	0.19	0.11	0.12	0.16	0.30	0.15	0.21	0.30
LFW connection ductility 6												
	q_{μ}				q_D				q			
Storeys	2	3	4	global	2	3	4	global	2	3	4	global
Min	1.2	1.3	1.2	1.2	1.2	1.0	1.0	1.0	1.6	1.6	1.4	1.4
Mean	2.1	1.6	1.7	1.8	1.4	1.1	1.2	1.2	2.8	1.8	2.2	2.3
Max	2.7	2.3	2.3	2.7	1.4	1.4	1.5	1.5	3.6	2.2	3.4	3.6
CoV	0.23	0.18	0.20	0.23	0.05	0.12	0.17	0.14	0.22	0.11	0.30	0.29
LFW connection ductility 8												
	q_{μ}				q_D				q			
Storeys	2	3	4	global	2	3	4	global	2	3	4	global
Min	1.5	1.5	1.4	1.4	1.3	1.1	1.1	1.1	2.4	2.1	1.7	1.7
Mean	2.3	1.8	2.0	2.0	1.6	1.3	1.3	1.4	3.8	2.4	2.6	2.9
Max	3.7	2.7	2.6	3.7	2.1	1.5	1.5	2.1	6.3	2.9	3.6	6.3
CoV	0.29	0.20	0.19	0.25	0.21	0.12	0.11	0.20	0.36	0.13	0.24	0.36

However, it is not possible to perform a direct comparison between these values and those provided by codes. In this study, the overstrength factor for the sheathing-to-frame connection was set to 1. Though, it is possible to multiply the intrinsic q by 1.5, which is the q -factor suggested by Eurocode 8 for a global non-dissipative behaviour, in order to calculate the q_{code} (code dependent q -factor)(Table 4).

Table 4: Mean value of the q_{code} factor for each ductility class.

Ductility Class	Storeys			global
	2	3	4	
4	3.6	2.6	2.4	2.9
6	4.3	2.8	3.3	3.4
8	5.6	3.6	4.0	4.4

For a ductility class equal to 4, a value of 2.9 was obtained, which confirms the $q=3$ provided by the Italian building code [27] for Low Ductility Class timber structures. On the other hand, a value of 3.4 was obtained for a ductility class 6, which is widely lower than 5, value suggested for Ductility Class High (DCH) by Eurocode 8 [6] and Italian Building Code [27]. Even a ductility class 8 is not sufficient to comply with Eurocode provision (a mean intrinsic q equal to 2.9, and a q -factor equal to 4.4). It is worth noticing that, in this work, all the dissipation is concentrated in the sheathing-to-frame connection, and the contribution of hold-downs and shear brackets are not taken in to account.

7 CONCLUSIONS

In this work, an Incremental Dynamic Analysis approach was used, in order to evaluate the behaviour factor for Light Frame Wood structures. Compared to the non-linear static approach, the dynamic analysis considers the cyclic behaviour of the walls and the frequency of the ground motion.

Three example buildings were calculated according to Eurocode and Capacity Design. Starting from an experimental test on a full-scale LFW wall, a set of walls was obtained, varying the ductility of the sheathing-to-frame connection, and an IDAs procedure was applied to the building assembled with parameterized walls.

The obtained results confirm the behaviour factor for Low Ductility Class according to the Italian building code. However, the q -factor for High Ductility Class is lower than that provided by Eurocode 8.

The results presented belong to a larger study. In the next phases, the influence of the non-regularity of buildings will be investigated and a greater number of accelerograms and ductility classes will be considered, in order to expand the dataset.

ACKNOWLEDGEMENT

This research work was partly financed by the ReLUI Consortium (Italian University Network of Seismic Engineering Laboratories), within the frame of the ReLUI-DPC 2022-2024 project WP13 “Timber Structures – Code contributions”.

REFERENCES

- [1] Mishra A., Humpenöder F., Churkina G. et al.: Land use change and carbon emissions of a transformation to timber cities. *Nat Commun*13, 4889, 2022. <https://doi.org/10.1038/s41467-022-32244-w> www.nature.com/articles/s41467-022-32244-w
- [2] Safarik D., Elbrecht J., Miranda W.: State of Tall timber 2022, CTBUH (Council on Tall Buildings and Urban Habitat) Journal , 2022 Issue.
- [3] Filiatrault A., Christovasilis I.P., Wanitkorkul A., van de Lindt J.W.: Experimental seismic response of a full-scale light-frame wood building. *J Struct Eng*, 136(3):246–254, 2009.
- [4] Van de Lindt J.W., Pei S., Pryor S.E., Shimizu H., Isoda H.: Experimental seismic response of a full-scale six-story light-frame wood building. *J Struct Eng*,136(10):1262–1272, 2010.
- [5] Tomasi R., Casagrande D., Grossi P., Sartori T.: Shaking table tests on a three-storey timber building. *Proc Inst Civil Eng Struct Build*, 168(11):853–867, 2015. <https://doi.org/10.1680/jstbu.14.00026>
- [6] EN 1998-1:2013. Eurocode 8: design of structures for earthquake resistance part 1: general rules, seismic actions and rules for buildings. Brussels, Belgium: CEN, European Committee for Standardization, 2013.
- [7] Faggiano B., Sandoli A., Iovane G., Fragiaco M., Bedon C., Gubana A., Ceraldi C., Follesa M., Gattesco N., Giubileo C., Pio Lauriola M., Podestà S., Calderoni B.: The Italian instructions for the design, execution and control of timber constructions (CNR-DT 206 R1/2018). *Engineering Structures*, 253, art. no. 113753, 2022. DOI: 10.1016/j.engstruct.2021.113753
- [8] Rossi S., Giongo I., Casagrande D., Tomasi R., Piazza M.: Evaluation of the displacement ductility for the seismic design of light-frame wood buildings. *Bulletin of Earthquake Engineering*, 17 (9), pp. 5313 – 5338, 2019. DOI: 10.1007/s10518-019-00659-4
- [9] Demirci C., Malaga-Chuquitaype C., Macorini L.: Seismic shear and acceleration demands in multi-storey cross-laminated timber buildings. *Engineering Structures*, 198, 2019. doi/10.1016/j.engstruct.2019.109467
- [10] NZS 3603, New Zealand Timber Structures Standards, 1993
- [11] IBC, International Building code, 2021.
- [12] Canadian Standards Association CSA O86, 2014.
- [13] Gubana A., Tomasi G.: Results analysis of an experimental shear test on a light frame timber wall. Technical Report UNIUD 01, Reluis project 2010-2013 (in Italian), 2013.
- [14] Melotto M.: Wood-based in-plane strengthening solutions for the seismic retrofit of traditional timber floors in masonry buildings. Doctoral Thesis, University of Brescia, Italy, 2017, tutor Alessandra Gubana.
- [15] EN 1995-1-1:2005. Eurocode 5: design of timber structures—part 1-1: general—common rules and rules for building, 2013.
- [16] Casagrande D., Sartori T., Tomasi R.: Capacity design approach for multi-storey timber-frame buildings. In: INTER conference, Bath 2014
- [17] Vamvatsikos D., Cornell C.A.: Incremental dynamic analysis, *Earthquake Engineering and Structural Dynamics* 31(3): 491–514, 2002.
- [18] Iervolino I., Galasso C., Cosenza E.: REXEL: computer

- aided record selection for code-based seismic structural analysis. *Bulletin of Earthquake Engineering*, 8:339-362, 2009. DOI 10.1007/s10518-009-9146-1
- [19] Fajfar P.: Capacity Spectrum Method Based On Inelastic demand Spectra. *Earthquake Engineering And Structural Dynamics*, Vol. 28, 979-993, 1999.
- [20] Newmark N.M., Hall W.J.: *Earthquake Spectra and Design*. Earthquake Engineering Research Institute Monograph Series, 1982
- [21] Ceccotti A., Massari M., Pozza L.: Procedures for seismic characterization of traditional and modern wooden building types. *Int J Quality Res*, 10(1):47–70, 2016. doi:10.18421/IJQR10.01-02
- [22] Ceccotti A., Sandhaas C.: A proposal for a standard procedure to establish the seismic behaviour factor q of timber buildings. In: *Proceedings of the 11th world conference on timber engineering WCTE*, Riva del Garda, Italy, 2010.
- [23] Aloisio A., Alaggio R., Fragiocomo M.: Fragility functions and behavior factors estimation of multi-story cross-laminated timber structures characterized by an energy-dependent hysteretic model. *Earthquake Spectra*, 37(1):134-159, 2021. doi:[10.1177/8755293020936696](https://doi.org/10.1177/8755293020936696)
- [24] Mwafy A.M., Elnashai A.S.: Calibration of force reduction factors of RC buildings. *J Earthq Eng*, 6:239–73, 2002.
- [25] Fanaie N., Ezzatshoar S.: Studying the seismic behavior of gate braced frames by incremental dynamic analysis (IDA), *Journal of Constructional Steel Research*, 99:111-120, 2014. <https://doi.org/10.1016/j.jcsr.2014.04.008>.
- [26] Ogggi P., Gopikrishna K., Nagariya A.: Seismic behavior and response reduction factors for concrete moment-resisting frames. *Bull Earthquake Eng* 19:5643–5663, 2021. <https://doi.org/10.1007/s10518-021-01184-z>
- [27] Italian Building Code NTC 2018, Ministerial Decree of 17th January 2018, M.I.T., Rome, 2018 (in Italian).